THE DESIGN AND PERFORMANCE OF A CIRCUIT TO MEASURE THE TUNING ERROR OF SINGLE-SIDEBAND RADIO RECEIVERS

David Allen Jones

NAVAL POSTGRADUATE SCHOOL
Monterey, California

THESIS

THE DESIGN AND PERFORMANCE OF A
CIRCUIT TO MEASURE THE TUNING ERROR OF
SINGLE-SIDEBAND RADIO RECEIVERS

by

David Allan Jones

Thesis Advisor: G. Myers

September 1972

The Design and Performance of a Circuit to Measure the Tuning Error of Single-Sideband Radio Receivers

by

David Allan Jones
Lieutenant, United States Navy
B.S., University of Mississippi, 1965

Submitted in partial fulfillment of the
requirements for the degree of

MASTER OF SCIENCE IN ELECTRICAL ENGINEERING

from the

NAVAL POSTGRADUATE SCHOOL
September 1972

ABSTRACT

In order to automatically tune a single-sideband (SSB) radio receiver to the carrier frequency of a voice-modulated, suppressed-carrier, single-sideband radio signal, the difference between the frequency of the suppressed carrier and the frequency of the local oscillator in the receiver must be determined. A circuit which generates a sinusoidal voltage of the same frequency as the tuning error is examined analytically and experimentally. The design of the circuit is based on the principle that vowel sounds in human speech are periodic. The inputs to the circuit are the audio output of the SSB receiver for which the tuning error is desired and the audio output of an envelope detector which amplitude demodulates the SSB radio signal. The envelope detector provides a reference signal which is a harmonic of the fundamental modulating frequency of the SSB radio signal. This reference signal and the SSB receiver audio are non-linear processed to generate the error voltage. Receiver tuning errors as small as 0.1 Hertz were measured using this circuit.

TABLE OF CONTENTS

LIST OF FIGURES

I. INTRODUCTION

In single-sideband (SSB) communications, the carrier and one of the sidebands are suppressed. This provides two distinct advantages of single-sideband modulation as compared with double-sideband amplitude modulation (AM). The bandwidth required for transmission of a given signal by SSB is one-half the bandwidth required for transmission of the same signal by AM and less distortion is caused by the propogating medium because of the reduced bandwidth.

The primary disadvantage of SSB is the requirement for coherent detection to recover the modulating signal exactly. That is, the frequency and phase of the carrier must be known precisely at the receiver. This is a distinct problem since in SSB communications, the carrier is suppressed and not directly available at the receiver. In some communication systems this problem is avoided by inserting a portion of the carrier so that it is available at the receiver, at the expense of signal-to-noise ratio for a fixed amount of transmitter power available. There is a need for a system which is capable of determining the frequency and phase of the suppressed carrier without the sacrifice made by the insertion of a pilot carrier at the transmitter. In voice communications, since the human ear is insensitive to phase distortion, the problem reduces to determination of frequency alone. It is desirable to tune the receiver to this frequency without the aid of an operator.

Reference 1 investigates a method for the determination of the frequency of the suppressed carrier. The method utilizes information contained in the envelope of the transmitted signal. However, it requires that an operator observe a waveform on an oscilloscope and tune the receiver until a particular pattern is observed on the oscilloscope face. It is not apparent that this method can be used in the realization of a fully automatic system but the information contained in the envelope of the transmitted signal may be extracted by some other means to provide automatic operation.

This report investigates an experimental system which utilizes the envelope of the transmitted signal along with the normal product detected signal to generate an error signal when the modulating signal is periodic. This error signal has a waveform which can be converted to a control signal for fully automatic determination of the frequency of the suppressed carrier.

For the transmission of speech, the experimental system considered is based on the concepts that the envelope of the transmitted signal contains harmonics of the fundamental voice frequency of the speaker and that product detection of the transmitted signal provides information related to the fundamental voice frequency of the speaker and the receiver tuning error. A reference signal is generated by envelope detecting the transmitted signal and narrowband filtering to obtain a single harmonic of the fundamental voice frequency

of the speaker. The frequency of this harmonic is not affected by receiver tuning since it is assumed that the transmitted signal is in the passband of the receiver. Another signal is generated by product detecting the transmitted signal and narrowband filtering to obtain a signal whose frequency is a harmonic of the fundamental voice frequency of the speaker only if the local oscillator of the receiver is tuned to the frequency of the suppressed carrier. If the local oscillator of the receiver is not tuned to the frequency of the suppressed carrier, the signal passed by the narrowband filter differs in frequency from the harmonic of the fundamental voice frequency of the speaker by an amount equal to the receiver tuning error.

We now have two signals which together contain the essential information for the determination of the frequency of the suppressed carrier. Here we elect to do nonlinear processing, in the form of analog voltage multiplication, to extract the receiver tuning error. The envelope detector output and product detector output are multiplied and the result is lowpass filtered. The output of the lowpass filter is a sinusoidal signal whose frequency is equal to the receiver tuning error.

A detailed analysis of the predicted performance of the experimental system, for a periodic modulating signal, is contained in Chapter II. The results obtained by examining the performance of the experimental system are contained in Sections A and B of Chapter III. It is of interest to

observe the performance of the experimental system when the modulating signal is normal speech. Section C of Chapter III contains observations of interest for this case. A brief description of the experimental system and the equipment utilized in the verification of its performance is contained in Chapter IV. Conclusions and recommendations for further study are contained in Chapter V. Four appendices contain supporting analyses.

II. ANALYSIS OF THE EXPERIMENTAL SYSTEM

In this chapter we derive an expression for the error voltage, e(t), generated by the experimental system. We begin by reviewing some of the characteristics of human speech.

In general, human speech is random in nature. It is not possible to write an analytic expression which precisely represents human speech. However, the vowel sounds in human speech are periodic [Ref. 2, p. 323]. Consequently, these sounds can be represented by a sum of harmonically related sinusoidal terms of the form

$$a_1 \cos \omega_0 t + a_2 \cos 2\omega_0 t + \ldots + a_n \cos n\omega_0 t, \qquad (1)$$

where ω_0 is the fundamental voice frequency and $a_1, a_2, \ldots, a_n$ are constants.

The fundamental voice frequency, ω_0, is speaker dependent and is in the range from 90 Hertz to 250 Hertz. The fundamental voice frequency of an average adult male speaker is about 130 Hertz [Ref. 1, p. 19].

In the following derivation we assume a very simple, vowel-like sound which consists of a fundamental frequency, the third harmonic of the fundamental frequency and the sixth harmonic of the fundamental frequency. The coefficients a_1, a_3, and a_6 are assumed to be equal to one for simplicity. Thus the source signal v(t) has the form

$$v(t) = \cos \omega_0 t + \cos 3\omega_0 t + \cos 6\omega_0 t. \qquad (2)$$

The source signal, $v(t)$ is the voltage waveform of the input to the experimental system shown in block diagram form as Fig. 1.

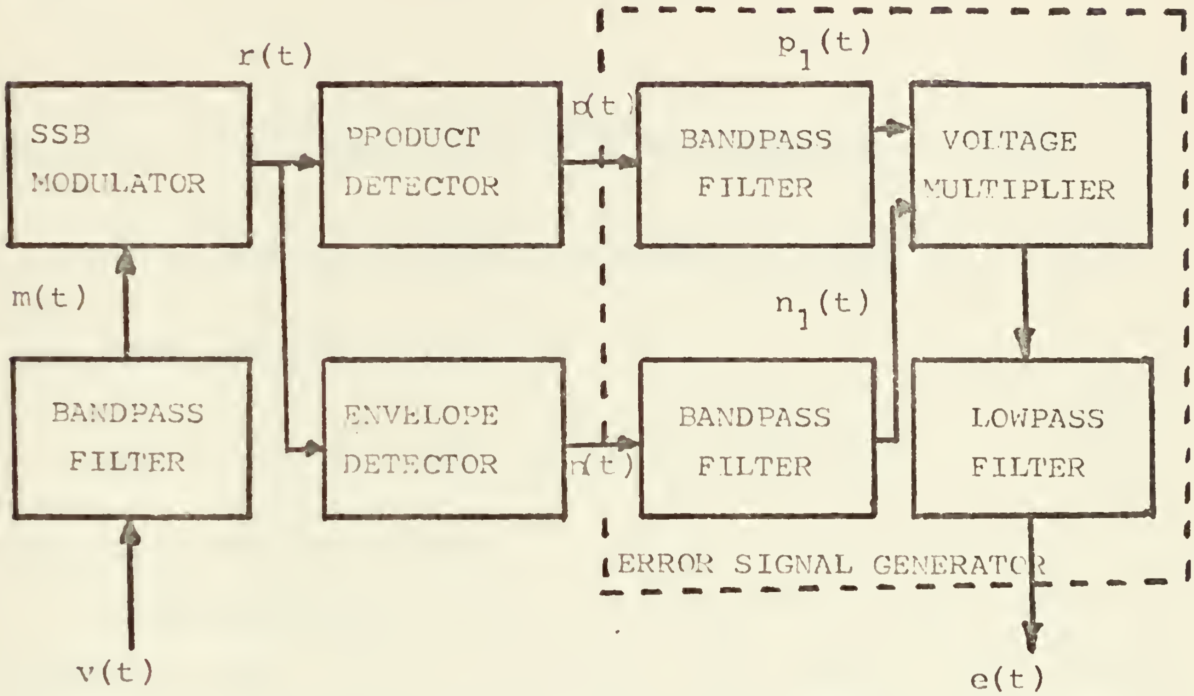

Figure 1. BLOCK DIAGRAM OF THE EXPERIMENTAL SYSTEM

A. SINGLE-SIDEBAND MODULATION AND DEMODULATION

In voice communication a bandpass filter is commonly used to limit the frequency range of the source signal. The band limits are typically 300 Hertz and 3500 Hertz which are compatible with the response of the human ear [Ref. 3, p. 61]. The message function $m(t)$ is obtained by passing the source signal, $v(t)$, through such a filter. Since $f_0 = \omega_0/2\pi$ is less than 300 Hertz, we obtain

$$m(t) = \cos 3\omega_0 t + \cos 6\omega_0 t. \tag{3}$$

1. Modulation

If the message function, $m(t)$, is used to single-sideband modulate a carrier function $c(t)$ of the form

$$c(t) = \cos \omega_c t, \tag{4}$$

it can be shown that the transmitted function is either

$$r(t) = \cos (\omega_c + 3\omega_0)t + \cos (\omega_c + 6\omega_0)t, \tag{5}$$

the upper-sideband signal or

$$q(t) = \cos (\omega_c - 3\omega_0)t + \cos (\omega_c - 6\omega_0)t, \tag{6}$$

the lower-sideband signal.

The transmitted function is assumed to be the upper-sideband signal, $r(t)$, throughout this report. The analysis of the lower-sideband signal, $q(t)$, is similar to that which follows.

2. Demodulation

Demodulation of a single-sideband signal is achieved by multiplying the received signal by an appropriate detection function and lowpass filtering.

If we assume that the received signal is the same as the transmitted function, $r(t)$, and that the detection function $d(t)$ is of the form

$$d(t) = 2 \cos \omega_d t, \tag{7}$$

multiplying $r(t)$ and $d(t)$ and lowpass filtering we obtain the product detected function $p(t)$ in the form

$$p(t) = \cos(\omega_c + 3\omega_0 - \omega_d)t + \cos(\omega_c + 6\omega_0 - \omega_d)t. \quad (8)$$

If ω_d is the same as ω_c, Eq. 8 reduces to

$$p(t) = \cos 3\omega_0 t + \cos 6\omega_0 t, \quad (9)$$

which is the same as the message function, m(t), in Eq. 2. However, since ω_c is not generally known precisely, there may be an error of the form

$$\delta = \omega_d - \omega_c \quad (10)$$

and Eq. 8 becomes

$$p(t) = \cos(3\omega_0 - \delta)t + \cos(6\omega_0 - \delta)t. \quad (11)$$

Since ω_d is the frequency of the local oscillator in the receiver and ω_c is the frequency of the suppressed carrier, δ is the receiver tuning error.

If we can determine δ by some means, we can find

$$\omega_d' = \omega_d - \delta. \quad (12)$$

Substituting Eq. 10 into Eq. 12 we obtain

$$\omega_d' = \omega_c. \quad (13)$$

If we change the detection function by retuning the receiver we obtain

$$d'(t) = 2\cos\omega_d' t \quad (14)$$

and Eq. 8 becomes

$$p(t) = \cos 3\omega_0 t + \cos 6\omega_0 t, \tag{15}$$

which is the same as the message function, m(t), in Eq. 2.

The remainder of this chapter is concerned with the determination of the receiver tuning error, δ.

B. DETERMINATION OF THE RECEIVER TUNING ERROR

It is shown in Appendix A that the envelope E(t) of the transmitted function, r(t) in Eq. 5, has the form

$$E(t) = 2 \cos \frac{3\omega_0}{2} t, \tag{16}$$

which is independent of ω_c, the suppressed carrier radian frequency.

The output of the envelope detector (full-wave rectifier), n(t), when excited by the received signal, which is assumed to be the same as the transmitted function, r(t), is the absolute value of E(t).

Utilizing the derivation of Appendix B, we find that

$$n(t) = \frac{4}{\pi} + \frac{4}{3\pi} \cos 3\omega_0 t - \frac{4}{7\pi} \cos 6\omega_0 t + \ldots + \frac{(-1)^{n+1} 4 \cos 3n\omega_0 t}{(4n^2-1)\pi}, \tag{17}$$

which is independent of ω_c, the frequency of the suppressed carrier, and ω_d, the frequency of the local oscillator in the receiver. This result is fundamental to the tuning method considered in this investigation. That is, since n(t) does not depend on ω_d, we can use n(t) as a reference

signal to indicate the correct frequencies of the sinusoidal components of the message function, m(t). The single sideband receiver is tuned until the frequencies of the sinusoidal components of p(t) exactly match those of n(t). This investigation, then, is concerned with means of determining when that match is effected.

After bandpass filtering p(t) in Eq. 11 and n(t) in Eq. 17, we obtain

$$p_1(t) = \cos\,(3\omega_0 - \delta)t \tag{18}$$

and

$$n_1(t) = \frac{4}{3\pi}\cos\,3\omega_0 t. \tag{19}$$

The error voltage e(t) is obtained by voltage multiplying

$$n_1(t)\cdot p_1(t) = \frac{2}{3\pi}\cos\,\delta t + \frac{2}{3\pi}\cos\,(6\omega_0 - \delta)t \tag{20}$$

and lowpass filtering which gives

$$e(t) = \frac{2}{3\pi}\cos\,\delta t, \tag{21}$$

a function of the difference of the suppressed-carrier frequency and the receiver local-oscillator frequency.

C. EXTENSION OF THE SIMPLE VOWEL MODEL

Based on the knowledge that vowel sounds can be represented by the expression in Eq. 1 and that the envelope detected function, n(t), is independent of ω_c and ω_d, we generalize the derivation of the error voltage, e(t), by

assuming that vowel sounds are sustained in normal speech such that the error voltage, e(t), is generated. We also assume that e(t) exists for a duration such that δ can be determined.

Since the average duration of vowel sounds is about 300 milliseconds in normal speech [Ref. 4, p. 121], and since we can expect the error voltage, e(t), to be of the form of Eq. 21 while vowel sounds are present, the minimum average tuning error that we can expect to detect is one which has a half-period of about 300 milliseconds. This places a theoretical limit of about 1.67 Hertz on the average minimum detectable tuning error when human speech is the source signal, v(t).

III. EXPERIMENTAL RESULTS

In this chapter, the performance of the experimental system is presented by considering the voltage waveforms at various points in the experimental system. Two different source signals are considered when the receiver tuning error is 10 Hertz and when the receiver tuning error is less than one Hertz. The two source signals are a two-tone message function and the sustained vowel sound, long $\bar{e}$ as in "b$\bar{e}$."
A block diagram of the experimental system, with the points labeled, is shown as Fig. 1 (Chapter II).

In addition to the two source signals above, it is of interest to observe the performance of the experimental system when the source signal is normal speech. This is done in Section C of this chapter.

Throughout this chapter, the upper oscilloscope trace of a two trace photograph is referred to as trace A and the lower trace is referred to as trace B.

A. TWO-TONE MESSAGE FUNCTION

The voltage waveforms of the message function, m(t), and the transmitted function, r(t), are shown in Fig. 2 as trace A and trace B respectively. The voltage waveforms

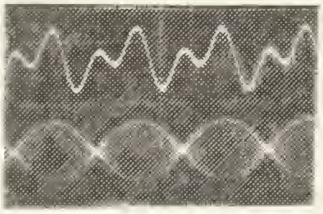

Figure 2. VOLTAGE WAVEFORMS OF m(t) AND r(t) FOR TWO-TONE MESSAGE FUNCTION

of the message function, m(t), and the transmitted function, r(t), are unaffected by receiver tuning.

The voltage waveforms of the product detected function, p(t), and the envelope detected function, n(t), are shown in Fig. 3 as trace A and trace B respectively.

(a) 10 Hertz Error (b) 0.2 Hertz Error

Figure 3. VOLTAGE WAVEFORMS OF p(t) AND n(t) FOR TWO-TONE MESSAGE FUNCTION

We observe that the period of p(t) (trace A) is slightly greater in Fig. 3(a) than in Fig. 3(b) which indicates that the sinusoidal terms are of different frequencies. We observe also that the period of m(t) (trace A of Fig. 2) is very nearly the same as the period of p(t) (trace A of Fig. 3(b)) when tuning error is small.

From the voltage waveforms of n(t), we observe that the period of n(t) is unaffected by receiver tuning error. The difference between the voltage waveform of n(t) and the envelope of the transmitted function, r(t), (trace B of Fig. 2) is attributed to the fact that the envelope detector is not designed to follow the envelope of an SSB signal.

The voltage waveforms of $p_1(t)$ and $n_1(t)$, the outputs of the narrowband filters of Fig. 1, are shown in Fig. 4(a) and 4(b) respectively. We observe in Fig. 4(a) that the frequency

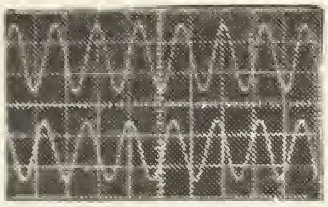

(a) 10 Hertz Error

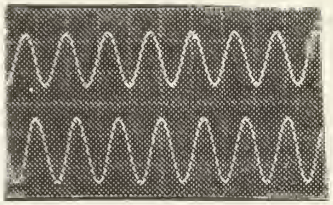

(b) 0.2 Hertz Error

Figure 4. VOLTAGE WAVEFORMS OF $p_1(t)$ AND $n_1(t)$ FOR TWO-TONE MESSAGE FUNCTION

of $p_1(t)$ is different from the frequency of $n_1(t)$ while in Fig. 4(b) the frequencies are very nearly the same. Using a frequency counter, the frequency difference observed in Fig. 4(a) is found to be 10 Hertz, which is the same as the receiver tuning error.

The voltage waveform of the error voltage, e(t), is shown as Fig. 5. We observe that e(t) is sinusoidal and

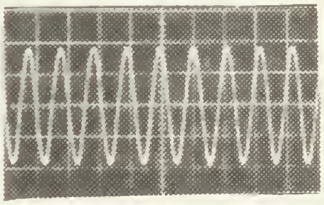

(a) 10 Hertz Error

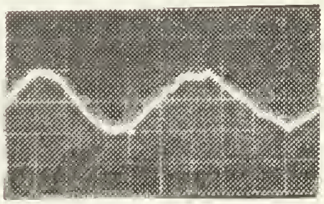

(b) 0.2 Hertz Error

Figure 5. VOLTAGE WAVEFORM OF e(t) FOR TWO-TONE MESSAGE FUNCTION

and that the frequency of e(t) is equal to the receiver tuning error.

Therefore, for the two-tone message function, we observe that the experimental system performs as predicted. Using

the experimental system with the two-tone message function, tuning errors as small as 0.1 Hertz are measured. This ability to measure small tuning errors suggests use of the system to determine frequency changes, such as doppler shift, which occur during transmission.

B. SUSTAINED VOWEL SOUND

For the sustained vowel sound long $\bar{e}$ as in "b$\bar{e}$," the voltage waveforms of the message function, m(t), and the transmitted function, r(t), are shown in Fig. 6 as trace A and trace B respectively. As with the two-tone message

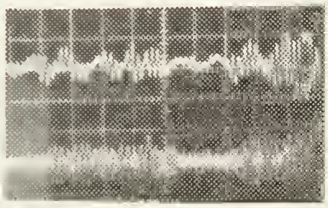

Figure 6. VOLTAGE WAVEFORMS OF m(t) AND r(t) FOR SUSTAINED VOWEL SOUND

function, these waveforms are unaffected by receiver tuning.

The voltage waveforms of the product detected function, p(t), and the envelope detected function, n(t), are shown in Fig. 7 as trace A and trace B respectively.

(a) 10 Hertz Error

(b) 0.5 Hertz Error

Figure 7. VOLTAGE WAVEFORMS OF p(t) AND n(t) FOR SUSTAINED VOWEL SOUND

We observe that the period of p(t) (trace A) is greater in Fig. 7(a) than in Fig. 7(b) which indicates that the sinusoidal terms are of different frequencies. We observe also that the period of m(t) (trace A of Fig. 6) is very nearly the same as the period of p(t) in the case of small tuning error (trace A of Fig. 7(b)).

The period of n(t) is observed to be unaffected by receiver tuning. The distortion of n(t) when compared with the envelope of r(t) (trace B of Fig. 6) is again attributed to the design of the envelope detector.

The voltage waveforms of $p_1(t)$ and $n_1(t)$, the outputs of the narrowband filters of Fig. 1, are shown in Fig. 8 as trace A and trace B respectively. The frequency of

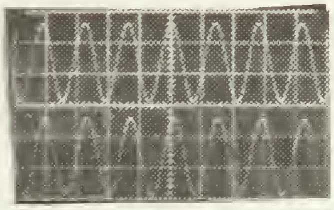

(a) 10 Hertz Error

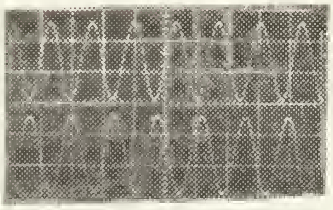

(b) 0.5 Hertz Error

Figure 8. VOLTAGE WAVEFORMS OF $p_1(t)$ and $n_1(t)$ FOR SUSTAINED VOWEL SOUND

$p_1(t)$ in Fig. 8(a) is observed to differ from the frequency, of $n_1(t)$ in Fig. 8(a) by 10 Hertz, the receiver tuning error, while the frequency of $p_1(t)$ and $n_1(t)$ are very nearly the same in Fig. 8(b).

The voltage waveform of the error voltage, e(t), is shown as Fig. 9. We observe that e(t) is sinusoidal and

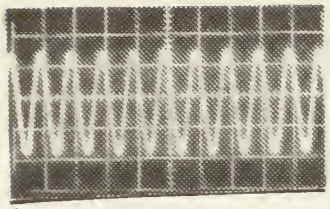

(a) 10 Hertz Error

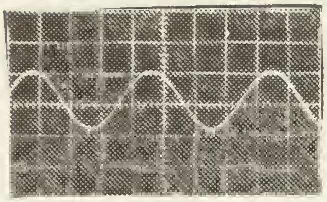

(b) 0.5 Hertz Error

Figure 9. VOLTAGE WAVEFORM OF e(t) FOR SUSTAINED VOWEL SOUND

that the frequency of e(t) is equal to the receiver tuning error. Therefore, for the sustained vowel sound, we observe that the experimental system performs as predicted. Using the experimental system with the sustained vowel sound, tuning errors as small as 0.4 Hertz are measured.

C. SPEECH

In this section we observe the performance of the experimental system when the source signal is human speech. The error voltage is not sinusoidal since the modulating voltage is not periodic. However, it is observed that the reference signal $n_1(t)$ is sinusoidal and its frequency is a harmonic of the fundamental voice frequency of the speaker. Figure 10 is the voltage waveform of $n_1(t)$ when the modulating signal is speech.

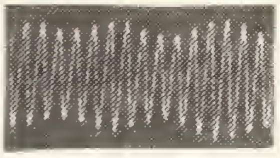

Figure 10. VOLTAGE WAVEFORM OF $n_1(t)$ FOR SPEECH

For vowel sounds, it is observed that the magnitude of the envelope of $n_1(t)$ increases. Further, this envelope is approximately constant for the duration of the vowel sound.

IV. EXPERIMENTAL APPARATUS

This chapter describes the error signal generator and the equipment used to verify the performance of the experimental system.

A. THE ERROR SIGNAL GENERATOR

The error signal generator consists of two identical bandpass filters, an analog voltage multiplier and a lowpass filter connected as shown in Fig. 11.

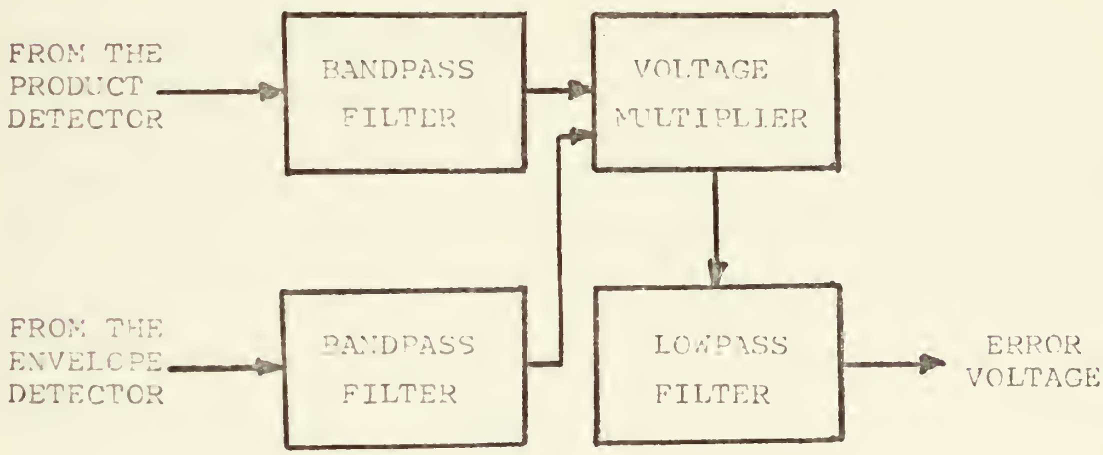

Figure 11. BLOCK DIAGRAM OF THE ERROR SIGNAL GENERATOR

1. The Bandpass Filters

The bandpass filters are six pole elliptical filters with a center frequency of 350 Hertz and a bandwidth 100

Hertz. Since the operating frequencies of the filters are relatively low, the filters are realized as active filters to avoid the use of large inductors normally associated with low-frequency filters. The operational amplifiers used in the realization of the filters are Signetics N5558 Dual Operational Amplifiers [Ref. 5, p. 65]. The synthesis of the bandpass filters is described in Appendix C.

2. The Voltage Multiplier

The voltage multiplier is a Hybrid Systems Corporation Model 107C analog multiplier/divider which requires no external components [Ref. 6]. The divide and square-root functions of the 107C are not used in this application.

3. The Lowpass Filter

The lowpass filter is a fith-order Butterworth lowpass filter. A cut-off frequency of 30 Hertz is selected since it is assumed that the receiver is tuned to within 30 Hertz of the carrier frequency prior to the utilization of the error signal generator. The synthesis of the lowpass filter is described in Appendix D.

B. THE SINGLE-SIDEBAND MODULATOR

The single-sideband modulator is a T-827/URT radio transmitter, which is the transmitter of the Radio Set AN/WRC-1B, operated in the upper-sideband mode. It has an operating range of 2.0 to 29.9995 megahertz and employs digital tuning to automatically tune to any one of 280,000 channels in 100 Hertz steps. The frequency generation

circuits are referenced to a stable master oscillator with a stability better than 1 part in 10^8 per day [Ref. 7].

C. THE PRODUCT DETECTOR

The product detector is an R-1051B/URR radio receiver which is operated in the upper-sideband mode. It has an operating range of 2.0 to 30.0 megahertz and employs digital tuning to automatically tune to any one of 280,000 channels in 100 Hertz steps. Like the single-sideband modulator, the product detector has frequency generating circuits which are referenced to a stable master oscillator with a stability better than 1 part in 10^8 per day. Optional vernier tuning is provided for continuous tuning over a 1.0 kilohertz range [Ref. 7].

In the vernier tuning mode, the receiver frequency may be calculated to within one Hertz by measuring the frequency of the vernier oscillator. By modifying the vernier tuning circuit as shown in Appendix A of Ref. 1, the receiver frequency may be calculated to within 0.33 Hertz. This allows determination of the receiver tuning error to within 0.33 Hertz. Smaller errors are measured by observing the error voltage e(t) trace on the oscilloscope face.

D. THE ENVELOPE DETECTOR

The envelope detector is another R-1051B/URR radio receiver. Since the time constants of the diode detector

in the R-1051B/URR are not designed to follow the envelope of a single-sideband signal, some distortion is introduced.

E. OTHER EQUIPMENT

The oscilloscope is a general purpose laboratory oscilloscope (Tektronix 531A). Single-sweep triggering is achieved by applying a short duration pulse to the external sweep-triggering input to obtain photographs.

Two signal generators (Wavetex 142) are used to generate the two-tone message function by summing the output of each signal generator with the operational amplifier mixer shown as Fig. 12.

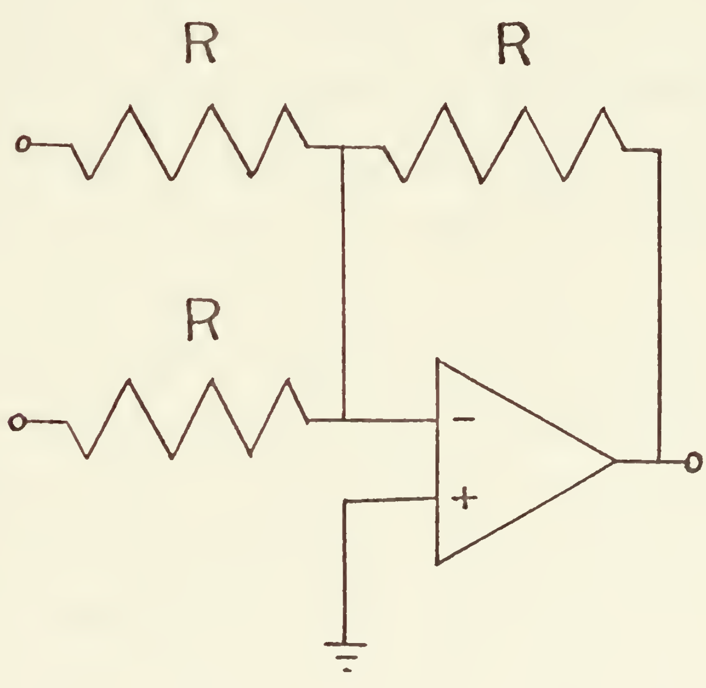

Figure 12. THE TWO-TONE GENERATOR

V. CONCLUSIONS AND RECOMMENDATIONS

A. CONCLUSIONS

We have shown that a single-sideband modulated signal contains all of the necessary information for determining the frequency of the suppressed carrier when the modulating signal is periodic. The experimental system has been demonstrated to be capable of extracting the receiver tuning error by nonlinear processing of the single-sideband modulated signal. Errors as small as 0.1 Hertz were measured.

The results of this investigation lead to the following conclusions:

(1) Since the output of the experimental system is sinusoidal for a periodic modulating signal, it can be used to automatically tune the receiver to the frequency of the suppressed carrier by frequency detecting, level adjusting and applying the resultant d.c. level to a voltage controlled oscillator in the receiver.

(2) The detectable frequency error is inversely proportional to the duration of the periodic modulating signal.

(3) Given a means to gate the two demodulated signals into the error signal generator whenever vowel sounds are present, the experimental system might be used to automatically tune the receiver when the modulating signal is normal speech. The detectable frequency error then becomes limited by the duration of the vowel sounds.

B. RECOMMENDATIONS FOR FURTHER STUDY

This investigation was limited to one form of nonlinear processing of the single-sideband modulated signal. Linear processing may be used to better advantage to automatically tune the SSB receiver.

Two topics of interest which require further investigation are suggested below.

(1) It is observed that the envelope detected signal is distorted due to the design of the demodulator. It is suggested that an amplitude demodulator can be designed which will follow accurately the envelope of the SSB signal.

(2) It is observed that the outputs of the narrowband filters are amplitude modulated when the modulating signal is normal speech. It is suggested that hard limiting of these outputs might result in improved performance of the experimental system with speech as the modulating signal.

APPENDIX A

DERIVATION OF THE EXPRESSION FOR THE ENVELOPE OF THE TRANSMITTED FUNCTION

Beginning with the expression for the transmitted function

$$r(t) = \cos\ (\omega_c+3\omega_0)t + \cos\ (\omega_c+6\omega_0)t\ , \tag{A1}$$

we form the Hilbert transform

$$\hat{r}(t) = \sin\ (\omega_c+3\omega_0)t + \sin\ (\omega_c+6\omega_0)t\ , \tag{A2}$$

As shown in Ref. 3, the envelope E(t) of a function r(t) is

$$E(t) = [r^2(t) + \hat{r}^2(t)]^{1/2}\ . \tag{A3}$$

We find that

$$r^2(t) = \cos^2\ (\omega_c+3\omega_0)t + \cos^2\ (\omega_c+6\omega_0)t$$

$$+ 2\cos\ (\omega_c+3\omega_0)t\ \cos\ (\omega_c+6\omega_0)t \tag{A4}$$

and

$$\hat{r}^2(t) = \sin^2\ (\omega_c+3\omega_0)t + \cos^2(\omega_c+6\omega_0)t$$

$$+ 2\sin\ (\omega_c+3\omega_0)t\ \sin\ (\omega_c+6\omega_0)t\ . \tag{A5}$$

Taking the sum of Equations (A4) and (A5) and using trigonometric substitution, we find

$$r^2(t) + \hat{r}^2(t) = 2(1 + \cos\ 3\omega_0 t)\ . \tag{A6}$$

Further trigonometric substitution yields

$$E(t) = 2 \cos \frac{3\omega_0}{2} t \quad , \tag{A7}$$

the envelope of the transmitted function r(t).

APPENDIX B

DETERMINATION OF THE ABSOLUTE VALUE OF cos x

The function, $|\cos x|$, can be written as the product of cos x and an appropriate square wave. Using the Fourier cosine series expansion for a square wave of amplitude of plus one or minus one and period of 2π, we can write

$$|\cos x| = \frac{2}{\pi} + \sum_{n=1}^{\infty} \frac{(-1)^{n+1}\, 4 \cos 2nx}{(4n^2-1)\pi} \quad . \tag{B1}$$

APPENDIX C

SYNTHESIS OF THE BANDPASS FILTERS

We want to synthesize two, identical bandpass filters with the following characteristics: (1) center frequency of 350 Hertz; (2) bandwidth of 100 Hertz; (3) transmission zeros at zero Hertz, 245 Hertz, 455 Hertz and 700 Hertz; and (4) stopband attenuation at least 40 db below that of the passband.

Utilizing the IBM 360/67 Scientific Library Subroutine LISA, a six pole elliptical filter with the transfer function

$$H(s) = \frac{s_o(s_o^2 + 4.0)(s_o^2 + .49)(s_o^2 + 1.69)}{(s_o^2 + .1s_o + 1)(s_o^2 + .03s_o + .74)(s_o^2 + .02s_o + 1.3)}, \tag{C1}$$

where $s_o = s/\omega$ and $\omega = 2\pi(350)$, is found to meet all the design criteria.

To realize the filters, we first look at the four factors of Eq. C1. Three of them have the form

$$H_n(s) = -\frac{(\frac{s}{\omega})^2 + a_n^2}{(\frac{s}{\omega})^2 + b_n(\frac{s}{\omega}) + c_n^2} \tag{C2}$$

for n = 2,3 and 4. The other factor $H_1(s)$ has the form

$$H_1(s) = -\frac{s}{\omega} \quad . \tag{C3}$$

The transfer function $H_1(s)$ is observed to be the transfer function of the differentiator circuit shown as Fig. C1, where $RC = 1/\omega$.

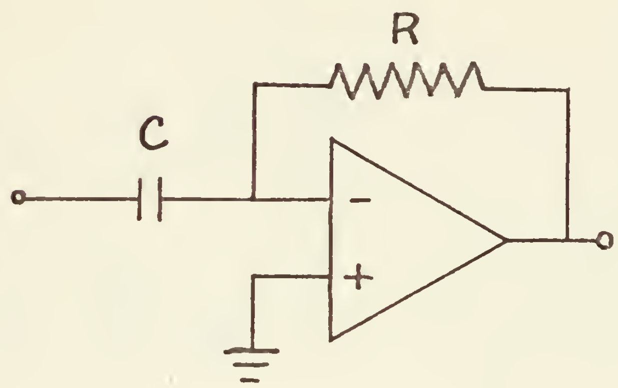

Figure C1. CIRCUIT DIAGRAM OF SECTION ONE OF THE BANDPASS FILTER

$H_n(s)$ is in the biquadratic form. The circuit diagram of a biquadratic section is shown in Fig. C2.

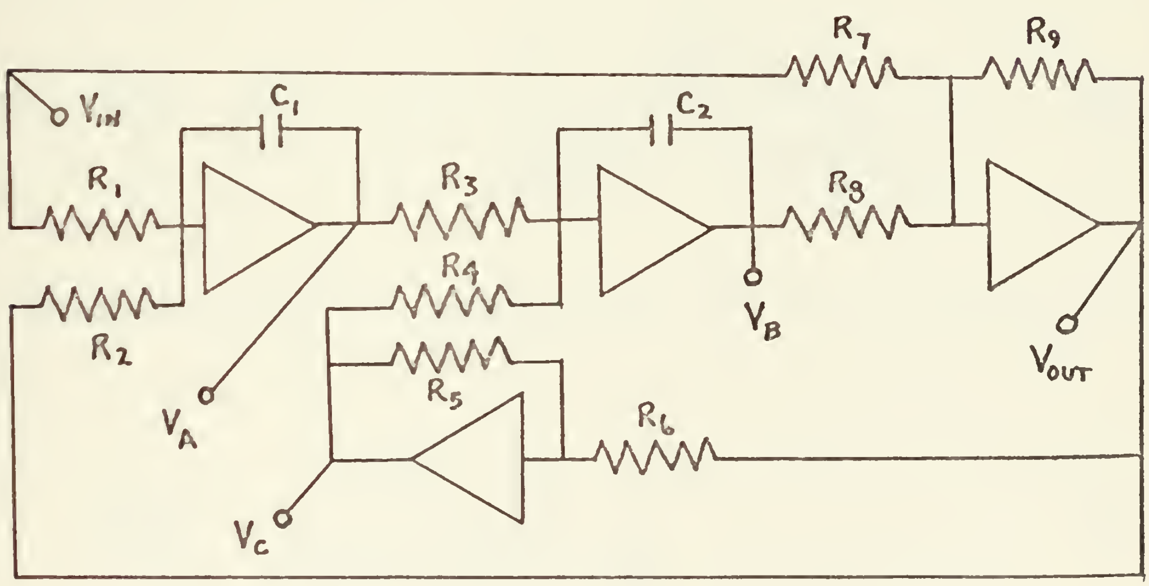

Figure C2. CIRCUIT DIAGRAM OF THE BIQUADRATIC SECTION

By observation,

$$V_A = -\frac{1}{sC_1}\left(\frac{V_{IN}}{R_1} + \frac{V_{OUT}}{R_2}\right), \tag{C4}$$

$$V_B = -\frac{1}{sC_2}\left(\frac{V_A}{R_3} + \frac{V_C}{R_4}\right), \tag{C5}$$

$$V_C = -\frac{R_5}{R_6} V_{OUT}, \tag{C6}$$

and

$$V_{OUT} = -R_9\left(\frac{V_{IN}}{R_7} + \frac{V_B}{R_B}\right). \tag{C7}$$

Solving Eq. C4, C5, C6 and C7 simultaneously, we obtain

$$\frac{V_{OUT}}{V_{IN}} = -\frac{R_9}{R_7} \cdot \frac{s^2 + \frac{R_7}{C_1C_2R_1R_3R_8}}{s^2 + \frac{R_5R_9}{C_2R_4R_6R_8} s + \frac{R_9}{C_1C_2R_2R_3R_8}}. \tag{C8}$$

If we let $R_3=R_4=R_5=R_7=R_8=R_9=R$ and $C_1=C_2=C$, Eq. C8 reduces to

$$\frac{V_{OUT}}{V_{IN}} = -\frac{R^2C^2s^2 + \frac{R}{R_1}}{R^2C^2s^2 + \frac{R}{R_6} RCs + \frac{R}{R_2}}. \tag{C9}$$

Now if $RC = 1/\omega$, $a^2 = R/R_1$, $b = R/R_6$ and $c^2 = R/R_2$, then

$$\frac{V_{OUT}}{V_{IN}} = - \frac{(\frac{s}{\omega})^2 + a^2}{(\frac{s}{\omega})^2 + b(\frac{s}{\omega}) + c^2} \quad . \tag{C10}$$

Therefore, $H_n(s)$ is realized by the circuit shown as Fig. C2 with the component values properly selected.

We can now realize H(s) by cascading the four sections which we realized individually. Since we utilized operational amplifiers as the basic building blocks in the synthesis, we do not encounter impedance matching problems normally associated with cascade filter sections because the output impedances of the operational amplifiers are near zero ohms and the input impedances are on the order of kilohms.

Figure C3 is the plot of the magnitude of the frequency response of the synthesized filter. The vertical displacement is measured in decibels and the horizontal displacement in Hertz.

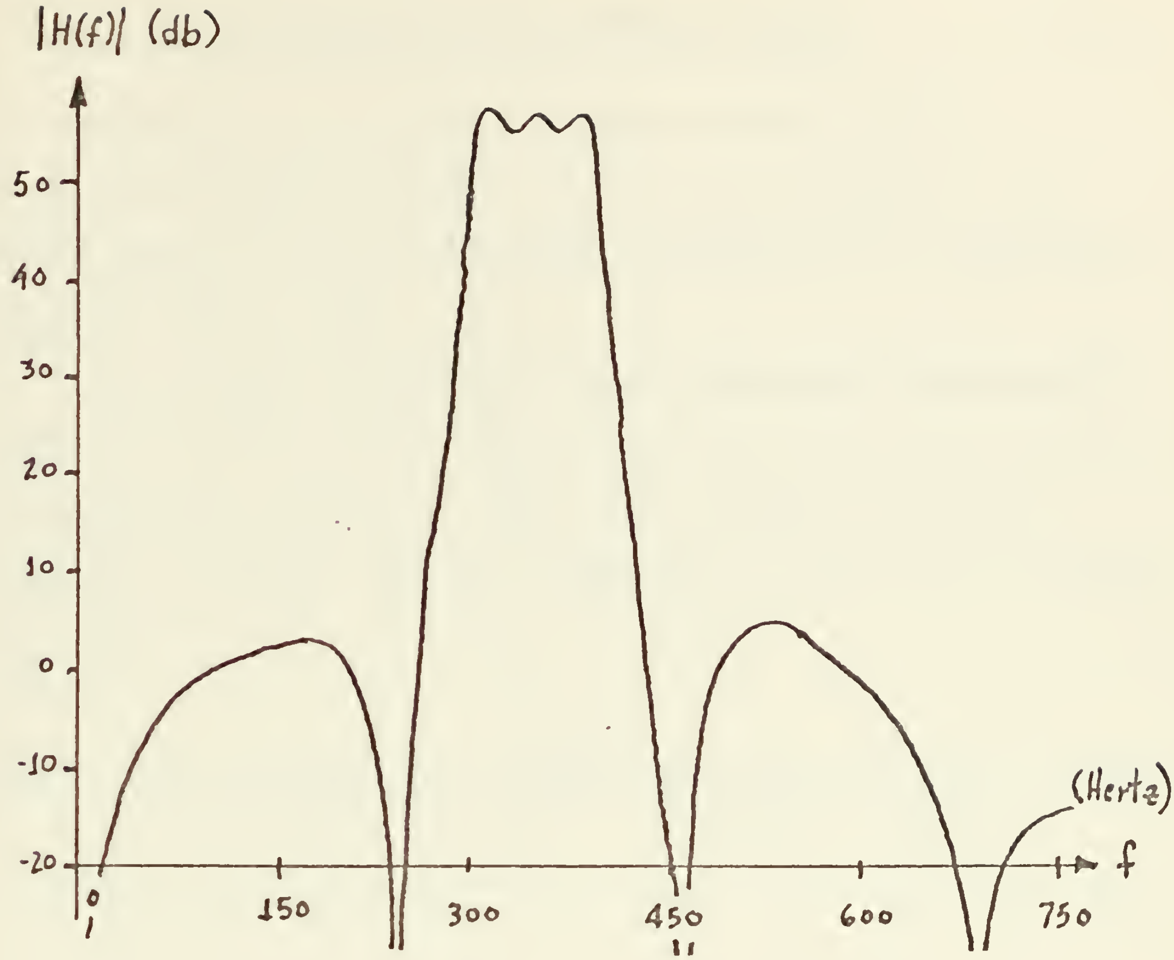

Figure C3. MAGNITUDE PLOT OF H(f) FOR THE BANDPASS FILTER

APPENDIX D

SYNTHESIS OF THE LOWPASS FILTER

We want to synthesize a lowpass filter with the following characteristics: (1) cut-off frequency of 30 Hertz; and (2) 100 db per decade attenuation of frequencies greater than cut-off.

Such a filter is found to be a fifth-order Butterworth filter [Ref. 8, p. 26]. Using the tabulated values for the capacitances [Ref. 8, p. 125], and frequency scaling to provide the proper cut-off frequency, we obtain the transfer function

$$H(s) = \frac{243.0}{s^5 + 9.708s^4 + 47.124s^3 + 141.372s^2 + 262.116s + 243.0} \quad \text{(D1)}$$

The realization of H(s) is shown in Fig. D1.

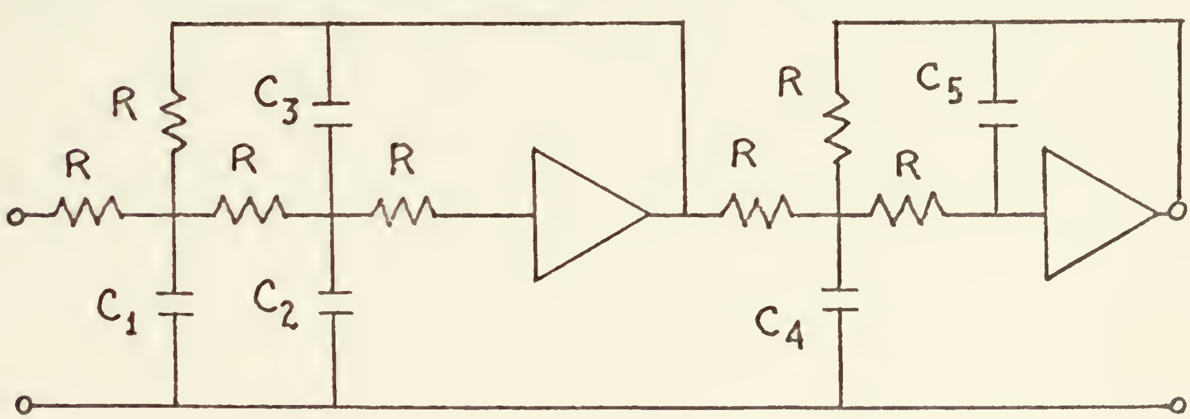

Figure D1. CIRCUIT DIAGRAM OF THE LOWPASS FILTER

Figure D2 is the plot of the magnitude of the frequency response of the synthesized filter. The vertical displacement is measured in decibels and the horizontal displacement in Hertz.

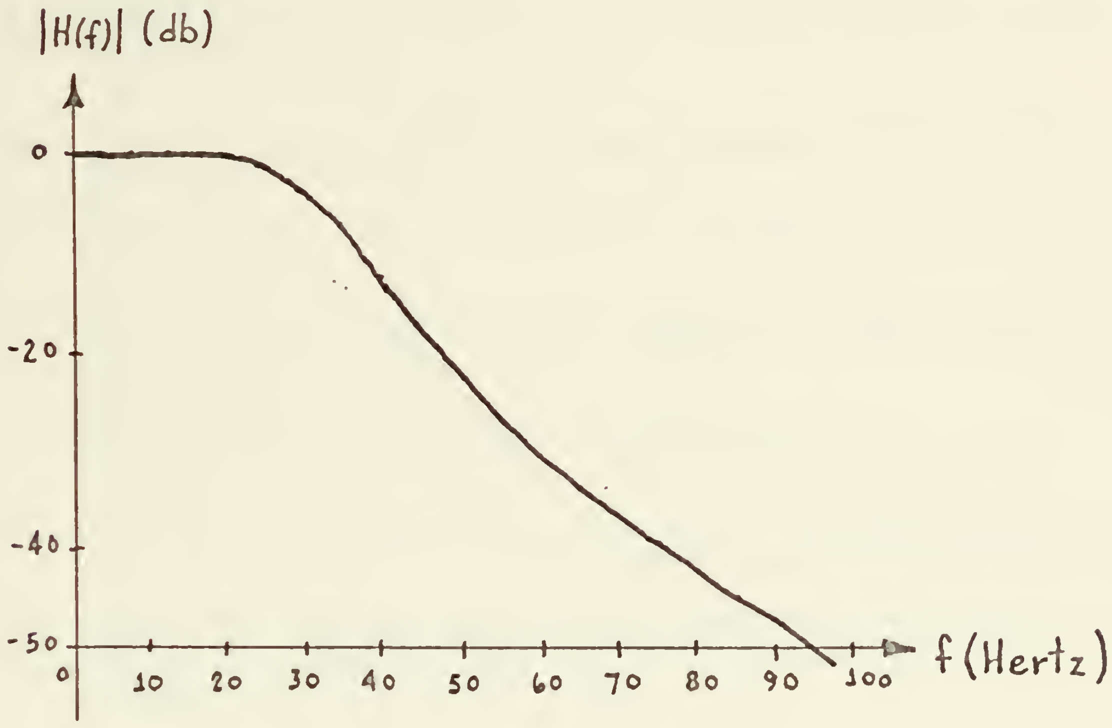

Figure D2. MAGNITUDE PLOT OF H(f) FOR THE LOWPASS FILTER

LIST OF REFERENCES

1. Day, L.B., Jr. and Myers, G.A., A Method for Accurate Receiver Tuning and Precise Measurement of the Carrier Frequency of Voice-Modulated, Suppressed-Carrier, Single-Sideband Radio Signals, TRNR-NPS-52MV71041A, Naval Postgraduate School, Monterey, 1971.

2. Papenfus, E. W., Bruene, W. B., and Schoenike, E. O., Single Sideband Principles and Circuits, McGraw-Hill, 1969.

3. Bennet, W. R., Introduction to Signal Transmission, McGraw-Hill, 1970.

4. Judson, L. S. and Weaver, A. T., Voice Science, F. S. Crofts, 1942.

5. Signetics Corporation D398 LIN-019-121 50M, Linear Integrated Circuits, Vol. 1, 1972.

6. Hybrid System Corporation Bulletin 107-2-1, Transconductance Analog Multiplier/Dividers, 1971.

7. Naval Ship System Command Technical Manual 0967-971-0010, Radio Set AN/WRC-1B and Antenna Coupler CU-937/UR, 1969.

8. Jover, H. M., Synthesis Techniques for Active RC Filters Using Operational Amplifiers, M. S. Thesis, Naval Postgraduate School, Monterey, 1970.

INITIAL DISTRIBUTION LIST

		No. Copies
1.	Defense Documentation Center Cameron Station Alexandria, Virginia 22314	2
2.	Library, Code 0212 Naval Postgraduate School Monterey, California 93940	2
3.	Associate Professor G. A. Myers, Code 52Mv Department of Electrical Engineering Naval Postgraduate School Monterey, California 93940	1
4.	LT David Allan Jones, USN, 261-62-7385/1110 U.S.S. HAMNER (DD-718) Fleet Post Office San Francisco, California 96601	1

DOCUMENT CONTROL DATA - R & D

(Security classification of title, body of abstract and indexing annotation must be entered when the overall report is classified)

1. ORIGINATING ACTIVITY (Corporate author)

Naval Postgraduate School
Monterey, California 93940

2a. REPORT SECURITY CLASSIFICATION

Unclassified

2b. GROUP

3. REPORT TITLE

The Design and Performance of a Circuit to Measure the Tuning Error of Single-Sideband Radio Receivers

4. DESCRIPTIVE NOTES (Type of report and, inclusive dates)

Master's Thesis; September 1972

5. AUTHOR(S) (First name, middle initial, last name)

David Allan Jones

6. REPORT DATE	7a. TOTAL NO. OF PAGES	7b. NO. OF REFS
September 1972	43	8

8a. CONTRACT OR GRANT NO.

b. PROJECT NO.

c.

d.

9a. ORIGINATOR'S REPORT NUMBER(S)

9b. OTHER REPORT NO(S) (Any other numbers that may be assigned this report)

10. DISTRIBUTION STATEMENT

Approved for public release; distribution unlimited.

11. SUPPLEMENTARY NOTES

12. SPONSORING MILITARY ACTIVITY

Naval Postgraduate School
Monterey, California 93940

13. ABSTRACT

In order to automatically tune a single-sideband (SSB) radio receiver to the carrier frequency of a voice-modulated, suppressed-carrier, single-sideband radio signal, the difference between the frequency of the suppressed carrier and the frequency of the local oscillator in the receiver must be determined. A circuit which generates a sinusoidal voltage of the same frequency as the tuning error is examined analytically and experimentally. The design of the circuit is based on the principle that vowel sounds in human speech are periodic. The inputs to the circuit are the audio output of the SSB receiver for which the tuning error is desired and the audio output of an envelope detector which amplitude demodulates the SSB radio signal. The envelope detector provides a reference signal which is a harmonic of the fundamental modulating frequency of the SSB radio signal. This reference signal and the SSB receiver audio are nonlinear processed to generate the error voltage. Receiver tuning erros as small as 0.1 Hertz were measured using this circuit.

14 KEY WORDS	LINK A		LINK B		LINK C	
	ROLE	WT	ROLE	WT	ROLE	WT
Receiver Tuning						
Voice Communication						
Single-Sideband Communication						
Frequency Measurement						
Frequency Monitoring						
Signal Monitoring						
Single-Sideband Receivers						
Speech Characteristics						

Thesis 138016
J693 Jones
c.1 The design and performance of a circuit to measure the tuning error of single-sideband radio receivers.